

RADGEN 1.0

Monte Carlo Generator for Radiative Events in DIS on Polarized and Unpolarized Targets

I.Akushevich^a, H.Böttcher^b, D.Ryckbosch^c

^a NC PHEP, Bogdanovich str. 153, 220040 Minsk, Belarus

^b DESY Zeuthen, 15738 Zeuthen, Germany

^c University of Gent, 9000 Gent, Belgium

Abstract: A new Monte-Carlo generator including real radiated photons in DIS on polarized and unpolarized targets is presented. Analytical and numerical tests are performed and discussed in details.

1 Introduction

Experimental data on lepton-nucleon scattering contain contributions from the usual Born process and from QED radiative effects which come from loop corrections and from processes with the emission of additional real photons. Any Monte-Carlo program simulating the experimental situation has to take into account these radiative processes by generating radiated photons because radiative corrections can be very large.

Depending on the four-momentum transfer squared (Q^2) and the energy transfer (ν) there are three basic channels for lepton scattering on nuclei, namely elastic, quasielastic, and inelastic processes. In the case of elastic scattering ($\nu = Q^2/2M_A$, where M_A is nuclear mass) the leptons are scattered off the nucleus leaving the nucleus in its ground state. Quasielastic scattering ($\nu \sim Q^2/2M$, where M is nucleon mass) corresponds roughly to direct collisions with the individual nucleons inside the nuclei. The inelastic scattering occurs when the pion threshold is reached ($\nu \geq Q^2/2M + m_\pi$ where m_π is the pion mass). At the Born level both Q^2 and ν are fixed completely by measuring the scattering angle and the energy (momentum) of the scattered lepton. However, at the level of radiative corrections, in case of presence of real radiated photons, the fixation is removed and the four-momentum of the radiated photon has to be included in the kinematical variable calculation. Such elastic, quasielastic and inelastic processes with radiation of a real photon are known as radiative tails from the elastic (σ_{el}) and the quasielastic (σ_q) peaks and from the continuous spectrum (σ_{in}) called hereafter shortly elastic, quasielastic and inelastic radiative tail.

The total radiative correction at the lowest order is obtained as the sum of these contributions together with loop corrections (σ_v) coming from effects of vacuum polarization and exchange of an additional virtual photon:

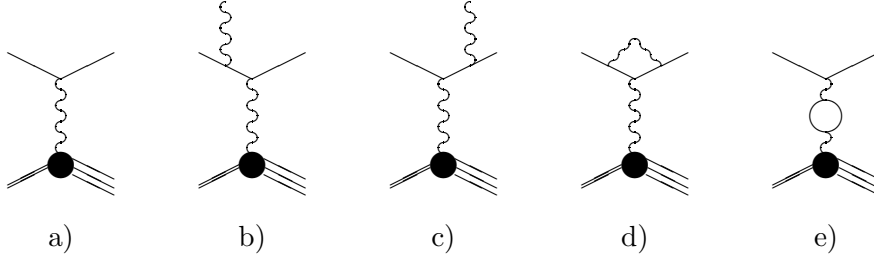


Figure 1: Feynman diagrams contributing to the Born and the radiative correction cross sections in lepton-nucleus scattering.

$$\sigma^{rad.corr.} = \sigma_{in} + \sigma_q + \sigma_{el} + \sigma_v. \quad (1)$$

In this report we present a Monte-Carlo generator for events with a possible radiation of a real photon in deep inelastic lepton scattering (DIS) on polarized and unpolarized targets. It should be noted that only the single photon exchange (no Z^0 exchange) and only pure QED corrections are considered. Hence the use of the generator is at present restricted to experiments where the electroweak contributions and corrections are small, as e.g. in the experiment HERMES at DESY. The events are generated in accordance with their contribution to the observed total cross section given by

$$\sigma_{obs} = \sigma_{non-rad}(\Delta) + \sigma_{in}(\Delta) + \sigma_q + \sigma_{el}. \quad (2)$$

The first term $\sigma_{non-rad}(\Delta)$ contains not only the contribution from the Born process but also the contributions from loop corrections (σ_v) and from multiple soft photon production with a total energy not exceeding a cut-off parameter Δ . In handling the radiative corrections two approaches have been used, the one developed by Mo and Tsai [1] and the one given by Bardin and Shumeiko [2]. These two formalisms and the significance of the cut-off parameter Δ will be discussed below in more detail. The generator contains two patches which can be considered as independent generators. The first one is based on the FORTRAN code POLRAD 2.0 [3] handling the polarized lepton-nucleon scattering. The other is based on FERRAD [4], a code that deals with the unpolarized case. They will be referred to as the POLRAD and FERRAD generator throughout the text. A detailed analytical and numerical comparison of the results given by the two generators is performed.

2 The Kinematics and Main Stages of Generation

The Feynman diagram for the Born (or one photon exchange) process is presented in Fig.1a. Its kinematics is completely defined by the scattering angle θ and the energy E' of the scattered lepton, two variables which are usually measured. All other inclusive kinematical variables can be expressed in terms of θ and E' . Having in mind the laboratory frame, i.e. the frame with the target nucleus at rest the relevant variables are

$$\begin{aligned} Q^2 &= 4EE' \sin^2 \frac{\theta}{2}, & \nu &= E - E', & x &= \frac{Q^2}{2M\nu}, \\ y &= \frac{\nu}{E}, & W^2 &= Q^2(1/x - 1) + M^2, \end{aligned} \quad (3)$$

where E is the beam energy, Q^2 is the negative of the four-momentum transfer squared, ν the energy transfer, x the Bjorken scaling variable, y the normalized energy transfer, and W^2 the mass squared of the hadronic final state. Radiative QED corrections (RC) at the lowest order are described by the set of the Feynman graphs shown in fig. 1b-e. Contributions to the lowest order RC cross section come from the diagrams b) and c) and from the interference of the loop diagrams d) and e) with the Born matrix element a).

An event registered in the detector with certain values of E' and θ for the scattered lepton can either be a non-radiative or a radiative event, i.e. an event containing a real hard radiated photon. For a radiative event there are apart from E' and θ three additional variables necessary to fix the kinematics of the radiated real photon. A possible choice is the photon energy E_γ and the two angles θ_γ and ϕ_γ , where θ_γ is the angle between the real and the virtual photon momenta \vec{k} and $\vec{q} = \vec{k}_1 - \vec{k}_2$ ($k_{1,2}$ being the momenta of the initial and the scattered lepton) and ϕ_γ is the angle between the planes defined by the momenta (\vec{k}_1, \vec{k}_2) and (\vec{k}, \vec{q}) . For events with the radiation of a real photon the kinematical variables describing the virtual photon and used to generate the hadronic final state differ from eq.(3) because the substitution $q \rightarrow q - k$ has to be made in their definition. The variables obtained after this substitution will be referred to as 'true' ones:

$$\begin{aligned} W_{true}^2 &= W^2 - 2E_\gamma(\nu + M - \sqrt{\nu^2 + Q^2} \cos \theta_\gamma), \quad \nu_{true} = \nu - E_\gamma, \\ Q_{true}^2 &= Q^2 + 2E_\gamma(\nu - \sqrt{\nu^2 + Q^2} \cos \theta_\gamma), \quad x_{true} = \frac{Q_{true}^2}{2M\nu_{true}}. \end{aligned} \quad (4)$$

For non-radiative events the true kinematics exactly coincide with (3).

In case of the elastic and quasielastic radiative processes the mass squared of the hadronic final state is fixed imposing additional constraints on the true kinematical variables. Indeed the following ranges are allowed:

$$\left\{ \begin{array}{ll} x \leq x_{true} \leq 1 & \text{for } \sigma_{in} \\ x_{true} = 1 & \text{for } \sigma_q \quad Q_{min}^2 \leq Q_{true}^2 \leq Q_{max}^2 \\ x_{true} = M_A/M & \text{for } \sigma_{el} \end{array} \right. \quad (5)$$

where

$$Q_{max,min}^2 = Q^2 \frac{2(1 - x_r)(1 \pm \sqrt{1 + \gamma^2}) + \gamma^2}{\gamma^2 + 4x_r(1 - x_r)} \quad (6)$$

and

$$\gamma^2 = 4M^2 x^2 / Q^2, \quad x_r = x / x_{true}. \quad (7)$$

The Monte-Carlo procedure for the generation of events with a possible photon radiation is as follows:

It starts off with the generation of the kinematics of the scattered lepton and the calculation of an event weight from these kinematics. Then the appropriate scattering channel (non-radiative; elastic, quasielastic or inelastic radiative tail) has to be chosen according to their contribution to the total observed cross section (see (2)). If a radiative channel is selected the radiated photon has to be generated and the values of the kinematical variables have to be re-computed

in order to obtain the true values. For each event the weight has to be recalculated. The new weight is defined as the ratio of the radiatively corrected and the Born cross section. After this recalculation the weighted sum of all events (generated originally in accordance with the Born cross section) gives the observed cross section.

The recalculation of the weight requires the knowledge of the cross section integrated over the photon momentum. This is done differently in the two theoretical approaches which will be discussed in detail in the subsections below. In the Mo-Tsai approach an additional parameter Δ is introduced dividing the integration region into a soft and a hard photonic part. No such parameter is used in the Bardin-Shumeiko approach. However, in both approaches a minimal photon energy E_{min}^γ is adapted in generating a radiated photon. Only if the photon energy is above this value the kinematics of the photon is calculated and the event becomes a radiative one. The actual value of E_{min}^γ depends on the aim of the photon generator. In general photons should be detected in the calorimeter. So the energy threshold of the calorimeter sets the value for E_{min}^γ .

In addition one needs spin averaged and spin dependent structure functions, quasielastic suppression factors and elastic formfactors to calculate the Born and observed cross sections. This is taken either from fits to experimental data or from model predictions. A recent 8-parameter fit from ref.[5] for the proton and deuterium structure function $F_2^{p,d}(x, Q^2)$ and their combination for ^3He ($F_2^{^3\text{He}} = \frac{1}{3}F_2^p + \frac{2}{3}F_2^d$) has been used. The spin dependent structure function $g_1(x, Q^2)$ is constructed from a fit to the spin asymmetry A_1 [3] according to

$$g_1(x, Q^2) = A_1(x)F_1(x, Q^2) = \frac{A_1(x)F_2(x, Q^2)}{2x(1 + R(x, Q^2))}(1 + \gamma^2). \quad (8)$$

For the structure function $R(x, Q^2)$ being the ratio of longitudinal to transverse virtual photon absorption cross sections Whitlow's fit [6] was used and assumed to be A-independent. No contributions are assumed from the spin dependent structure function $g_2(x, Q^2)$. For the elastic formfactors a fit to experimental data [7] is utilized. The quasielastic radiative tail is calculated in accordance with ref.[8]. In contrast to the elastic case where the treatment is exact (within the considered order of perturbative theory) here the Y-scaling hypothesis [9] and the peaking approximation (quasielastic structure functions are evaluated at the quasielastic peak) are applied.

The two Monte Carlo generators for radiative events available in RADGEN for the unpolarized and polarized cases are described below. The theoretical approaches, the approximations made, and the dependence of the radiative corrections on the artificial parameter Δ and on the value of the photon detector threshold E_{min}^γ are discussed.

2.1 The generator for the unpolarized case

The unpolarized generator is based on the FORTRAN code FERRAD35 [4]. The code calculates the radiative correction to deep inelastic scattering of unpolarized particles in accordance with the analytical formulae given by Mo and Tsai [1].

The result for the lowest order radiative correction of the cross section is

$$\sigma = \delta_R(\Delta)(1 + \delta_{vert} + \delta_{vac} + \delta_{sm})\sigma_{1\gamma} + \sigma_{el} + \sigma_q + \sigma_{in}(\Delta), \quad (9)$$

where $\sigma_{1\gamma}$ is the one photon exchange Born cross section and δ_{vac} , δ_{vert} , and δ_{sm} are corrections due to vacuum polarization by electron and muon pairs, vertex corrections and residuum of the cancellation of infrared divergent terms independent of Δ :

$$\begin{aligned}\delta_{vac} &= \frac{\alpha}{\pi} \left[-\frac{20}{9} + \frac{2}{3} \ln \frac{Q^2}{m_e^2} + \frac{2}{3} \ln \frac{Q^2}{m_\mu^2} \right], \\ \delta_{vert} &= \frac{\alpha}{\pi} \left[-2 + \frac{3}{2} \ln \frac{Q^2}{m^2} \right], \\ \delta_{sm} &= \frac{\alpha}{\pi} \left[-\frac{\pi^2}{6} + \text{Li}_2\left(\cos^2 \frac{\theta}{2}\right) - \frac{1}{2} \ln^2(1-y) \right],\end{aligned}\tag{10}$$

where m is the lepton mass and $\text{Li}_2(x) = -\int_0^x dy \ln(1-y)/y$ is the dilogarithm or Spence function.

The cross sections σ_{el} , σ_q , and σ_{in} are the contributions from radiative processes (i.e. including real photon radiation) for elastic, quasielastic and deep inelastic scattering. They can be calculated in terms of the radiative tail from the j th mass level σ_j

$$\sigma_{el} = \sigma_{el}(M_A, 1), \quad \sigma_q = \sigma_q(M, 1), \quad \sigma_{in} = \int_{M+m_\pi}^W dM_h \sigma_{in}(M_h, \theta_{max}),\tag{11}$$

where $M_h = \sqrt{W_{true}^2}$ and σ_j ($j = el, q, in$) has the form of an integral over θ_γ , the angle between the real and the virtual photons:

$$\sigma_j(M, \theta_{max}) = \int_0^{\theta_{max}} d\theta_\gamma T_0(W_2^j(T_1 + T_2 + T_3 + T_4 + T_5) + W_1^j(T_6 + T_7)).\tag{12}$$

The explicit form of the structure functions $W_{1,2}^j$ depends on the type of the tail. The terms T_i are kinematical factors (see ref.[1] for details). The integration limit θ_{max} is defined as $\theta_{max} = \min(\pi, \theta_\Delta)$ where θ_Δ can be found from the relation

$$W_{true}^2 = W^2 - 2\Delta(\nu + M - \sqrt{\nu^2 + Q^2} \cos(\theta_\Delta)).\tag{13}$$

An artificial parameter Δ had to be introduced to divide the integration region over the photon energy into two parts, the soft and the hard energy regions. The hard energy region $\sigma_{in}(\Delta)$ can be calculated without any approximations. The soft photon part is calculated for photon energies approaching zero. After cancellation of the infrared divergences and a resummation of soft multiphoton effects the correction factor is given by

$$\delta_R(\Delta) = \exp \left[-\frac{\alpha}{\pi} \left(\ln \frac{E}{\Delta} + \ln \frac{E'}{\Delta} \right) \left(\ln \frac{Q^2}{m^2} - 1 \right) \right].\tag{14}$$

Note that we follow ref.[1] in fixing that part of the soft photon correction which should be exponentiated. Another possible variant is the well-known prescription of ref.[10]. The dependence on Δ is the deficiency of the method. On the one hand this artificial parameter has to be chosen sufficiently large to avoid numerical instabilities because for $\Delta = 0$ the contribution $\sigma_{in}(\Delta)$ gets infinite. On the other hand it has to be chosen sufficiently small to reduce the soft photon region which is calculated only approximately. If the threshold over the photon energy is low enough, it is customary to use the same value for the parameters Δ and E_{min}^γ .

2.2 The generator for the polarized case

The polarized generator is constructed utilizing the FORTRAN code POLRAD 2.0 [3, 11]. This code is based on the method of covariant cancellation of infrared divergences developed by Bardin and Shumeiko [2]. The final formula for the cross section free of infrared divergences does not include any artificial parameter like Δ . However, E_{min}^γ has to be introduced if the code is used considering the generation of real radiated photons. The cross section formula of ref.[11] can be rewritten into a form similar to eq.(9):

$$\sigma = \delta_R(E_{min}^\gamma)(1 + \delta_{vert} + \delta_{vac} + \delta_{sm})\sigma_{1\gamma} + \sigma_{add}(E_{min}^\gamma) + \sigma_{el} + \sigma_q + \sigma_{in}(E_{min}^\gamma). \quad (15)$$

In the ultrarelativistic approximation ($Q^2 \gg m^2$) the corrections δ_{vert} , δ_{vac} , and δ_{sm} take the same form as in eq.(10)¹. The covariant form of the radiative tails for a nuclear target with atomic number A is as follows:

$$\begin{aligned} \sigma_{in} &= -\alpha^3 y \int_{\tau_{min}}^{\tau_{max}} d\tau \sum_{i=1}^4 \sum_{j=1}^{k_i} \theta_{ij}(\tau) \int_{R_{min}}^{R_{max}} dR \frac{R^{j-2}}{(Q^2 + R\tau)^2} \mathfrak{S}_i(R, \tau), \\ \sigma_{el} &= -\frac{\alpha^3 y}{A^2} \int_{\tau_{Amin}}^{\tau_{Amax}} d\tau_A \sum_{i=1}^4 \sum_{j=1}^{k_i} \theta_{ij}(\tau_A) \frac{2M_A^2 R_{elA}^{j-2}}{(1 + \tau_A)(Q^2 + R_{elA}\tau_A)^2} \mathfrak{S}_i^{el}(R_{el}, \tau_A), \\ \sigma_q &= -\frac{\alpha^3 y}{A} \int_{\tau_{min}}^{\tau_{max}} d\tau \sum_{i=1}^4 \sum_{j=1}^{k_i} \theta_{ij}(\tau) \frac{2M^2 R_{el}^{j-2}}{(1 + \tau)(Q^2 + R_{el}\tau)^2} \mathfrak{S}_i^q(R_q, \tau). \end{aligned} \quad (16)$$

The integration limits are determined by $\tau_{max,min} = Q^2/2M^2x(1 \pm \sqrt{1 + 4M^2x^2/Q^2})$, $R_{min} = 2ME_{min}^\gamma$, and $R_{max} = (W^2 - (M + m_\pi)^2)/(1 + \tau)$. The quantities θ_{ij} are kinematical factors, and \mathfrak{S}_i are some combinations of the DIS structure functions, elastic formfactors or quasielastic response functions (see ref.[11] for details). The sum over i corresponds to contributions from spin averaged ($i = 1, 2$) and spin dependent ($i = 3, 4$) structure functions. In the case of the elastic and quasielastic radiative tail there is no integration over R because the R range is reduced to the constant values $R = R_{elA}$ and $R = R_{el}$ ($R_{el} = (2M\nu - Q^2)/(1 + \tau)$) due to the fixed final hadron mass. Invariants with the index "A" contain the nucleus momentum p_A instead of p ($p_A^2 = M_A^2$).

Apart from the usual ultrarelativistic approximation another one was made when the eqs. (9) and (14) were obtained, namely the photon energy was considered to be small $E^\gamma \ll E, E'$ in the region $E^\gamma < E_{min}^\gamma$. In POLRAD, the term $\sigma_{add}(E_{min}^\gamma)$ is added to take the difference of this approximation to the exact formula into account:

$$\begin{aligned} \sigma_{add}(E_{min}^\gamma) &= -\alpha^3 y \int_{\tau_{min}}^{\tau_{max}} d\tau \sum_{i=1}^4 \left\{ \theta_{i1}(\tau) \int_0^{2ME_{min}^\gamma} \frac{dR}{R} \left[\frac{\mathfrak{S}_i(R, \tau)}{(Q^2 + R\tau)^2} - \frac{\mathfrak{S}_i(0, 0)}{Q^4} \right] \right. \\ &\quad \left. + \sum_{j=2}^{k_i} \theta_{ij}(\tau) \int_0^{2ME_{min}^\gamma} dR \frac{R^{j-2}}{(Q^2 + R\tau)^2} \mathfrak{S}_i(R, \tau) \right\}. \end{aligned} \quad (17)$$

Therefore, the results obtained with the help of POLRAD are independent of the threshold parameter E_{min}^γ by construction.

¹It should be noted that contributions from τ -leptons and quark loops were included into δ_{vac} [11].

3 Comparison and Numerical Results

3.1 Analytical comparison

The expressions for the spin independent part of the radiative tails in eq. (16) have been compared analytically with the radiative tails given by eqs.(11) and (12) for the unpolarized case using the algebraic programming system REDUCE 3.5. It turned out that

$$\begin{aligned} -2M\sqrt{\nu^2 + Q^2} \sum_{j=1}^3 \Theta_{2i}(\tau) R^{j-3} &= T_1 + T_2 + T_3 + T_4 + T_5, \\ -2M\sqrt{\nu^2 + Q^2} \sum_{j=1}^3 \Theta_{1i}(\tau) R^{j-3} &= T_6 + T_7. \end{aligned} \quad (18)$$

From these relations one can easily show that the formulae for the radiative tails are exactly the same when no spin is considered.

All corresponding terms in (9) and (15) coincide exactly and there is only one additional term σ_{add} in eq. (15). This term can be considered as characterizing the quality of the soft photon approximation and can be calculated analytically by expanding it in the parameter $\epsilon = 2ME_{min}^\gamma/Q^2$:

$$\sigma_{add}(E_{min}^\gamma) = \epsilon \frac{\alpha}{\pi} \bar{\sigma}_0 - \epsilon \frac{\alpha^3 y}{Q^2} (\delta_\tau F_1 + \delta_{22} F_2) + O(\epsilon^2), \quad (19)$$

where $\bar{\sigma}_0$ is obtained in terms of the Born cross section σ_0 :

$$\bar{\sigma}_0 = \sigma_0 \begin{cases} F_1 \rightarrow J_0 x^2 \frac{\partial F_1}{\partial x} - \delta_\tau \left(-2F_1 + x \frac{\partial F_1}{\partial x} + Q^2 \frac{\partial F_1}{\partial Q^2} \right) \\ F_2 \rightarrow J_0 \left(x^2 \frac{\partial F_1}{\partial x} + x F_2 \right) - \delta_\tau \left(-2F_2 + x \frac{\partial F_2}{\partial x} + Q^2 \frac{\partial F_2}{\partial Q^2} \right). \end{cases} \quad (20)$$

The quantities J_0 , δ_τ , and δ_{22} depend only on kinematical variables:

$$\begin{aligned} \delta_\tau &= \frac{xy}{1-y} \left(1 - 2 \ln \frac{2E'}{m} \right) - xy \left(1 - 2 \ln \frac{2E}{m} \right), & J_0 &= 2 \left(\ln \frac{Q^2}{m^2} - 1 \right), \\ \delta_{22} &= -4 \frac{2-y}{y} \ln(1-y) - 2J_0 - \frac{4M^2 x}{Q^2} \delta_\tau. \end{aligned} \quad (21)$$

The first term in eq.(19) corresponds to the approximation $E_\gamma = 0$ in arguments of structure functions (terms with derivatives) and the photonic propagator (terms without derivative). The second term in eq.(19) appears when the approximation is applied to kinematical terms like $T_{1..7}$ as in eq.(12).

The numerical analysis performed for HERMES kinematics shows that the difference between both generators in the unpolarized case due to this additional contribution is negligible.

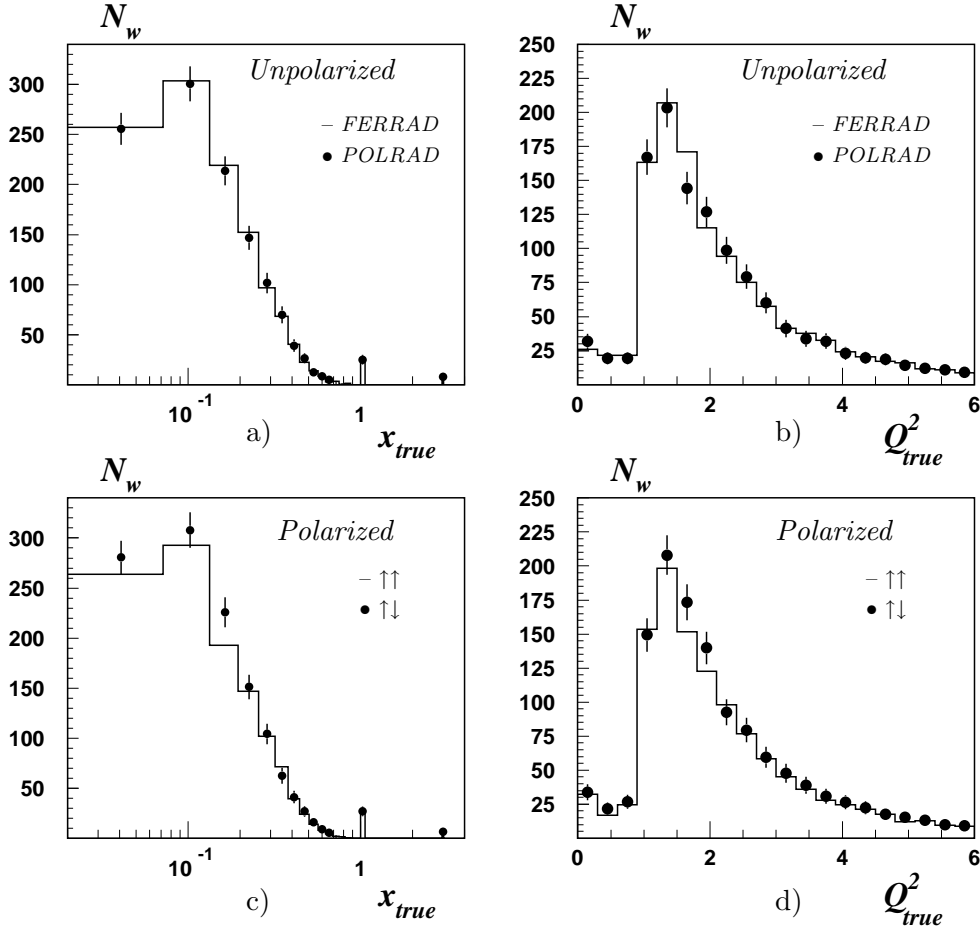


Figure 2: The weighted x_{true} and Q^2_{true} distributions as generated by FERRAD (histogram) and POLRAD with polarization part switched off (points) a), b); and by POLRAD with parallel (histogram) and antiparallel (points) spin configurations c), d).

3.2 Numerical comparison

In order to compare these two generators numerically Monte-Carlo event samples of 100k events each have been generated for a ^3He target and kinematical cuts relevant for the HERMES experiment [14] have been applied ($Q^2 > 1 \text{ GeV}^2$, $W^2 > 4 \text{ GeV}^2$, $y < 0.85$, $0.037 < \theta < 0.14 \text{ rad}$). Weighted distributions (N_w) of x_{true} and Q^2_{true} generated by the FERRAD and the POLRAD generators are shown in Fig.2. In Figs. 2a and 2b the unpolarized case is compared, i.e. FERRAD and POLRAD with the polarization part switched off. As can be seen the distributions are in agreement. It should be noted that the events at $x \approx 1$ and $x \approx 3$ correspond to the quasielastic and elastic radiative tails, respectively. In Fig. 2c) and 2d) a comparison of the parallel and antiparallel spin configuration in POLRAD is given. Here a systematic difference is seen which is expected from a spin asymmetry different from zero at small values of x .

The distributions of the radiation angles θ_γ and ϕ_γ as defined in the so-called Tsai-system in which the z -axis is along the direction of the virtual photon and the y -axis is normal to the scattering plane (see ref.[1]) and of the energy E_γ are displayed in Fig.3. These distributions are generated for a certain point in the kinematical plane of the scattered lepton, i.e. for x

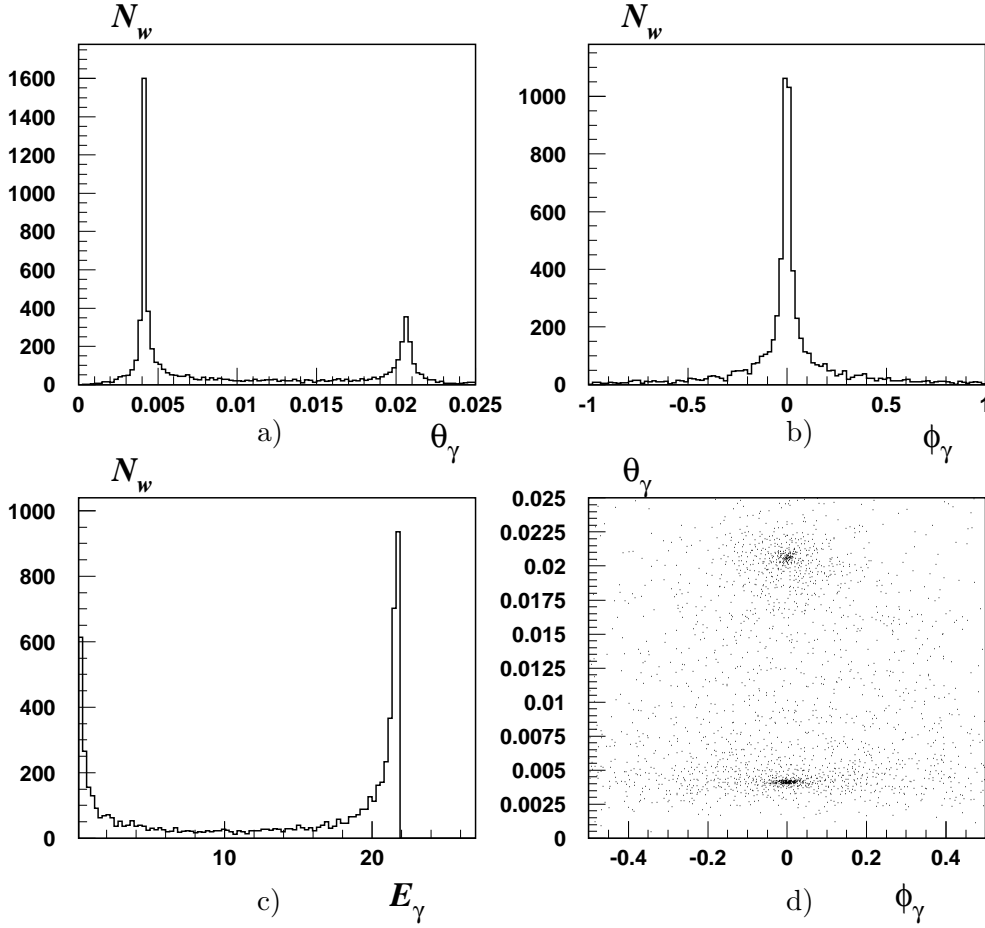


Figure 3: The distribution of the radiation angles θ_γ a) and ϕ_γ b) and of the energy c) of the radiated photon for $x = 0.1$ and $y = 0.8$. The two-dimensional distribution d) shows θ_γ vs ϕ_γ .

$= 0.1$ and $y = 0.8$. The two peaks seen in the θ_γ distribution of Fig.3 correspond to the s - and p -peak emerging from collinear radiation along the direction of the incoming and outgoing lepton, respectively.

Further results on the numerical comparison of the polarized and unpolarized case in the covariant and Mo-Tsai approach, respectively, can be found in the refs.[12, 13]. Fig.4 of ref. [13] presents the Δ -dependence of the radiative correction factor obtained by the code FERRAD. The general conclusion was that the best choice is Δ equal to about 0.1% of the beam energy. In this case the results should not depend on Δ .

The other task of the generators is to generate a radiative correction factor $\sigma_{obs}/\sigma_{Born}$ necessary to recalculate the weight of each event. A typical distribution of the RC factor is shown in Fig.4. Apart from this integration characteristics it is useful to consider also the behavior of the RC factor as a function of kinematical variables. Both the observed and Born cross sections can be split into spin averaged and spin dependent parts ($\sigma^{obs,Born} = \sigma_u^{obs,Born} + p_b p_t \sigma_p^{obs,Born}$, $p_{b,t}$ are beam and target polarizations) allowing to define the RC factors

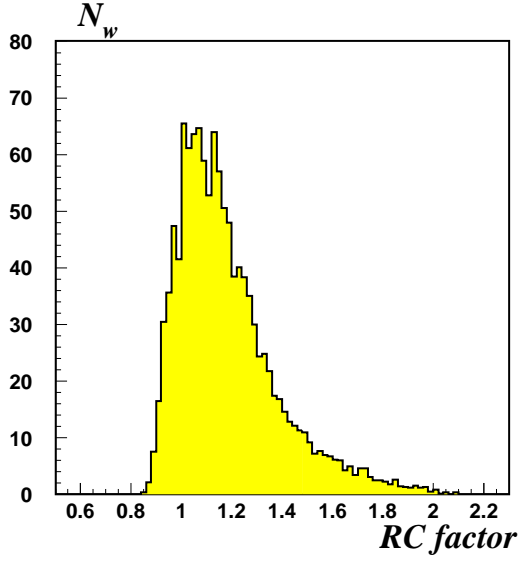


Figure 4: The typical distribution of the radiative correction factor.

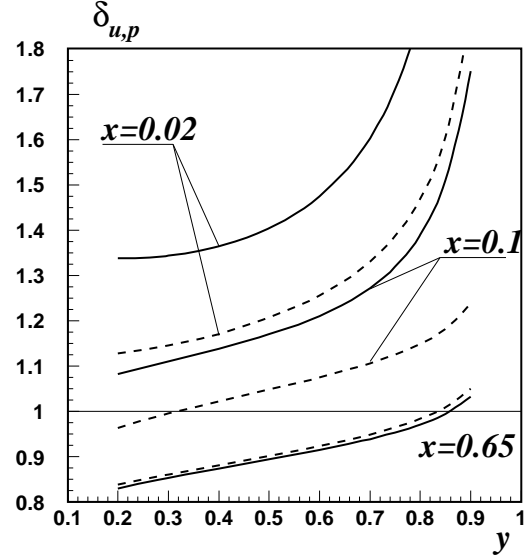


Figure 5: The spin averaged (full lines) and spin dependent (dashed lines) RC factor as a function of y for different values of x .

for the unpolarized and polarized case separately:

$$\delta_{u,p} = \frac{\sigma_{u,p}^{obs}}{\sigma_{u,p}^{Born}}. \quad (22)$$

Here we keep in mind that there is a region ($x \sim 0.4$ for ^3He case) where $\sigma_p^{Born}=0$. The y -dependence of these factors for several values of x is plotted in Fig.5. We would like to mention that the RC to the polarization asymmetry $A_{obs,Born} = \sigma_p^{obs,Born}/\sigma_u^{obs,Born}$ can be written in terms of $\delta_{u,p}$ as

$$\frac{A_{obs} - A_{Born}}{A_{Born}} = \frac{\delta_p - \delta_u}{\delta_u} \quad (23)$$

As can be seen from Fig.5 the correction factors δ_p and δ_u have similar behaviour and become almost equal with increasing x . The large corrections coming from the factorized part of eqs.(9) and (15) (the first term) cancel exactly in the numerator of (23) and only the unfactorized part of the corrections coming from the radiative tails contribute to the RC of the polarization asymmetry. This is the reason why there is a large correction to the total cross section and only a small one to the asymmetry.

4 Conclusion

The Monte-Carlo generator RADGEN 1.0 including radiative events in DIS on polarized and unpolarized targets have been presented. Two patches of the generator, one for the unpolarized case based on the FORTRAN code FERRAD35 and the other for the polarized case based on the FORTRAN code POLRAD 2.0 were compared and tested. This generator is implemented into the HERMES Monte-Carlo program HMC. The FORTRAN code of the Monte Carlo generator RADGEN 1.0 is available on request.

Acknowledgements

We are grateful to N.Shumeiko for help and support. We thank L.Favart and H.Spiesberger for their thoughtful comments that helped clarify the discussion in this paper. We would also like to thank N.Akopov, D.Bardin, N.Gagunashvili, P.Kuzhir, A.Nagaitsev for useful discussions and comments.

Appendix: Main options and keys

In this Appendix we briefly discuss options and keys which should be specified by a user in order to run RADGEN. They all are gathered in one input file 'input.dat' (default values are given in brackets):

- **nevent** [1000] – number of events;
- **ixytest** [0] – usage of look-up table for channel generation. The information about results of RC calculation in the 50×50 points over x and y is stored in this look-up table. The key defines the way how to use this information:
 - 1 two-dimensional spline
 - 2 FINT interpolation
 - 0 generation of the look-up table
 - 1 No use of the look-up table
- **ige** [2] – unpolarized (1) or polarized (2) generator is used;
- **ire** [1] – type of target: proton (1), deuteron (2), helium-3 (3);
- **e1** [27.5 GeV] – beam energy;
- **pl** and **pn** [0 and 0] – degrees of beam and target polarization;
- **ikkey** [0] – type of generation of leptonic kinematics
 - 1 – \mathbf{x} and \mathbf{y} are generated in accordance of the cross section within kinematical cuts,
 - 0 – \mathbf{x} and \mathbf{y} are read from the standard input;
- **ntk** [35] – number of bins in each of the seven parts of the integrand over the azimuthal photonic angle. The region over the azimuthal photonic angle is divided into seven parts in order to locate the peaks. This key defines the number of bins in each part of the integrand over the azimuthal photonic angle where the cross section is calculated.
- **nrr** [200] – number of bins in the integrand over photonic energy. This key defines the number of the bins over photon energy where cross section of the process is calculated and stored.
- **demin** [0.1 GeV] – Δ the threshold of photonic energy. Events with photonic energy smaller than Δ are considered as non-radiative.
- Kinematical cuts on y , x , Q^2 , W^2 , θ .

References

- [1] L.W.Mo and Y.S.Tsai, *Rev. Mod. Phys.* **41**, 205 (1969);
Y.S.Tsai, SLAC-PUB-848, 1971.
- [2] D.Bardin and N.Shumeiko, *Nucl. Phys. B* **127**, 242 (1977)
- [3] I.Akushevich, A.Ilyichev, N.Shumeiko, A.Soroko, A.Tolkachev, *Comp. Phys. Comm.* **104**, 201 (1997)
- [4] FERRAD 3.5 . This code was first created by J. Drees for EMC and further developed by M. Dueren.
- [5] NMC collaboration, *Nucl. Phys. B* **371**, 3 (1992)
- [6] K. Abe *et al.* [E143 Collaboration], hep-ex/9808028;
L.W. Whitlow, SLAC-report-357(1990)
- [7] J.S.McCarthy, I.Sick and R.R.Whitney, *Phys.Rev. C* **15**, 1396 (1977)
- [8] I.Akushevich, D.Ryckbosch, N.Shumeiko and A.Tolkachev, HERMES Internal Note 96-025, 1996.
- [9] A.K.Thompson et al., *Phys. Rev. Lett.* **68**, 2901 (1992)
- [10] D.R.Yennie, S.Frautchi, H.Suura, *Ann. Phys. (N. Y.)* **13**, 379 (1961)
- [11] I.V.Akushevich and N.M.Shumeiko, *J. Phys. G* **20**, 513 (1994)
- [12] P.P.Kuzhir, N.M.Shumeiko, *Sov.J.Nucl.Phys.* **55**, 1086 (1992)
- [13] B.Badelek, D.Bardin, K.Kurek and C.Scholz, *Z. Phys. C* **66**, 591 (1995)
- [14] K. Ackerstaff *et al.* [HERMES Collaboration], *Phys. Lett. B* **404**, 383 (1997)